View metadata, citation and similar papers at core.ac.uk
brought to you by CORE
provided by Revistas Universidad del Bío-Bío

ISSN online 0718-221X
maderas CIENCIA Y TECNOLOGIA, 12(2):115-125, 2010
DOI 10.4067/S0718-221X2010000200006

MODELING OF TRANSIENT MASS TRANSFER OF A GASEOUS COMPONENT IN AN ISOTHERMAL POROUS ADSORBENT

Anélie Pétrissans[1], Bajil Ouartassi[1], André Zoulalian[1], Mathieu Pétrissans [2]

ABSTRACT

The present study is avoided to a better understanding of the complexity of the adsorption process of a gaseous constituent on a porous solid (wood) with the purpose to improve the modeling. During the sorption on the porous solid, the diffusion mass transfer of the gaseous substance *A* occurs simultaneously in gaseous and adsorbed phases. The mass balance equations are written for the simultaneous diffusion transfers. The thermodynamic equilibrium between the phases is also represented. Four different models have been compared. Numerical results have been compared with experimental data and show that the hypothesis of equilibrium conditions between the gaseous and the adsorbed phases is not always verified.

Keywords: Adsorption, diffusion, mass transfer, modeling, porous solid, wood.

INTRODUCTION

The analysis of the sorption of gaseous substance in an isothermal porous solid without chemical reaction, involves the following steps (see Fig. 1).

a. Diffusionnel transfer of the adsorbate A in the gaseous phase, because of the existent concentration gradient.
b. Transfer of the adsorbate A from the bulk fluid to the surface of the porous solid.
c. Diffusionnel transfer of the gaseous constituent into the adsorbent pores.
d. Adsorption process.
e. Diffusionnel transfer of the adsorbed constituent in the adsorbent pores.

Classical chemical engineering models generally express the sorption processes on isothermal porous solid as a function of the adsorbed phase concentration gradient. They do not introduce the simultaneous diffusion of the constituent *A* in both the gaseous and the adsorbed phase (steps c and e). Furthermore, in addition to the diffusion of free molecules in the pore, adsorbed molecules can reveal mobile and slide from one site to another. This motion is known as surface diffusion. Moreover, the sorption processes are often considered with the hypothesis that the constituent in the adsorbed phase remain in thermodynamic equilibrium with the gaseous phase composition. Several workmanships have been developed about the fundamental principles of the adsorption processes, kinetic models and equilibrium studies (Ruthven 1984, Yang 1987, Do 1998). The multicomponent transient diffusion and the interaction and competition between the adsorbates have been studied by Do and Do (1998). The presence of viscous flow, resulting of the existence of partial pressure gradient and the heat effects during the adsorption were introduced in the models (Do and Do 1998, Mugge *et al*. 2001)

1LERMAB, UHP Nancy I, BP 239, 54506 Vandoeuvre les Nancy, Nancy. France
2LERMAB, Université Nancy 2, IUT Hubert Curien, 88000 Epinal, Epinal. France
Corresponding author: Anelie.Petrissans@lermab.uhp-nancy.fr
Received: 18.03. 2010. Accepted: 23.06. 2010.

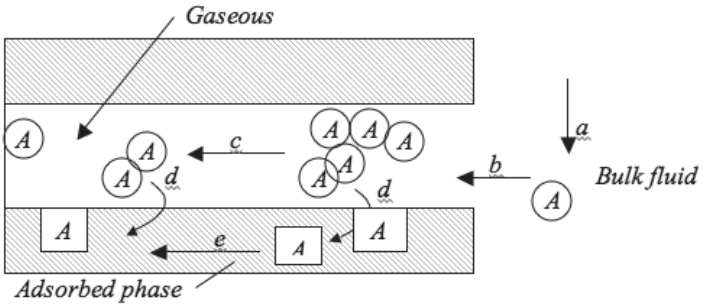

Fig. 1. Steps involved in the adsorption process.

This study is interested by the unsteady state modeling of the mass transfer of one gaseous adsorbate in a porous media during sorption process in isothermal conditions. The mass transfer is limited only to the diffusion; there is no internal convective transfer. In fact, in absence of a heat gradient the convective transfer of the gaseous phase is negligible. The porous media was considered as isotropic. This simplest representation of the pore structure of the adsorbent was proposed by Glueckauf and Coates (1947) and is well adapted for isothermal systems. In this model, diffusion flux is proportional to concentration gradient and an effectiveness diffusion coefficient which brings in the porosity of the system and the tortuosity of the pores. The diffusion transfer is supposed in only one direction. The numerical results obtained by the classical modeling and the models taking into account the simultaneous diffusion in gaseous and adsorbed phase are compared to the experimental data obtained for the desorption of vapor water. This example could be used in very restrictive conditions. In fact, this kind of sorption processes occurs during the slow processes of wood drying and humidification in the hydroscopic area. The analysis of this comparison allows study the importance of introducing the simultaneous diffusion fluxes. The existence of the thermodynamic equilibrium is also discussed in this paper. Four models are proposed in this work. The following hypothesis was used:

- Model I the mass of the adsorbate *A* in the gaseous phase in the pore of the solid sample is negligible comparing to the mass of *A* in the adsorbed phase. The diffusion of *A* in the porous solid is calculated using concentration gradient of *A* in the adsorbed phase and an apparent diffusion coefficient D^*. D^* is determined by optimization from the comparison between the theoretical and experimental curves and includes whole the diffusionnel transfer (Mouchot and Zoulalian 2005). Model I expresses the mass transfer using the optimized diffusion coefficient D^* and the concentration gradient of the constituent *A* in the adsorbed phase

- Model II reduces the process to the diffusion in the adsorbed phase only. The mass of the *A* in the gaseous phase in the pore of the solid sample is negligible and the diffusion flux of *A* in the gaseous phase is weak comparing to the diffusion process in the adsorbed phase. The transfer of *A* in gaseous phase was not introduced in this model. The adsorbed phase diffusion is characterized by a diffusion coefficient D_{Ads} which was measured independently (Mouchot and Zoulalian 2005).

- Model III the mass of *A* in the gaseous phase is taken into account. The diffusion transfers occur simultaneously in the gaseous and in the adsorbed phase. The corresponding diffusion coefficient D_V and D_{Ads} were determined by independent experimental devices (Mouchot and Zoulalian 2005). In this model the existence of a local thermodynamic equilibrium between the gaseous and in the adsorbed phase is assumed.

- Model IV the mass of *A* in the gaseous phase is also taken into account. Likewise the Model III, the diffusion transfers occur simultaneously in the gaseous and in the adsorbed phase but the thermodynamic

equilibrium between the two phases is not attended. In the absence of this equilibrium the flux φ of transferred adsorbate, is given by the equation (1):

$$\varphi = \rho_0 \; ka \, (f(\rho) - C) \qquad (1)$$

Where *C* is the solid phase concentration, expressed by the mass of *A* per unit mass of the solid before adsorption kg A.kg^{-1} porous solid, ρ is the density (kg.m^{-3}) of the constituent *A* in the gaseous phase related to the gas phase concentration *Cg* kg A.kg^{-1} vector gas, *f*(ρ) corresponds of the value of *C* in thermodynamic equilibrium with the mass of *A* in the surrounding gas, *ka* is a global volume transfer coefficient (s^{-1}), ρ_0 is the density of the porous solid before adsorption (kg.m^{-3}).

Mathematical formulation.

Let us consider an isotropic porous solid where the transfer of a gaseous adsorbate is limited in one principal direction. In these conditions, the analysis is based on the pellet model characterized by a contact surface *S* and thickness *e*. The sample presents symmetry with respect to the median plane perpendicular to the direction *y*. The thickness of the solid is very weak compared to the others dimensions. The transient mass balance equations describing the mass transfer of *A* using the four above listed models are given in the following paragraphs.

Mass balance equations relative to the Model I.

The mass balance equation of the transferred constituent *A* in the porous solid thickness ranging from *y* + *dy* to , are written :

$$-D^* \frac{\partial^2 C}{\partial y^2} + \frac{\partial C}{\partial t} = 0 \qquad (2)$$

The initial conditions are specified as follow:
at

$$t = 0 \qquad C = C_1 = f(\rho_1) \qquad (3)$$

The boundary conditions are given by:
at

$$y = 0 \qquad \frac{\partial C}{\partial y} = 0 \qquad (4)$$

at

$$y = e/2 \qquad C = C_2 = f(\rho_2) \qquad (5)$$

The boundary conditions (5), suppose that there is not any transfer resistance at the sample surface. If such transfer resistance exists, the boundary conditions are then substituted by the following expression:
at

$$y=e/2 \qquad -D^* \frac{\partial C}{\partial y} = h_m (C - f(\rho_2)) = h_m (C - C_2) \qquad (6)$$

When the boundary conditions (6) are used, the model is named Model Ia. The external transfer resistance will not be introduced in the Models II to IV.

Once the distribution of *A* over the sample thickness calculated numerically, the mass of the sample at any instant *t* can be evaluated by the equation (7).

$$m(t) = m_0 + 2\,S \int_0^{e/2} \rho_0\, C(t)\, dy \qquad (7)$$

where m_0 is the weigh of the sample before adsorption of *A*, *t* is the integration time, and *S* is the sample contact surface.

Mass balance equations relative to the Model II.

The mass balance equations of Model II are similar to the Model I equations. The difference comes from the consideration that the total diffusion transfer is realized in the adsorbed phase only. The diffusion process is characterized then by the diffusion coefficient in the adsorbed phase D_{Ads}. The mass balance equation of the adsorbed constituent *A* is given by (8):

$$-D_{Ads}\frac{\partial^2 C}{\partial y^2} + \frac{\partial C}{\partial t} = 0 \qquad (8)$$

The initial and the boundary conditions are identical given by the equations (3-5). The mass of the sample at each instant *t* is evaluated by the relation (7).

The comparison between the results obtained with the Model I and Model II allows understanding if the diffusion transfers of *A* could be reduced to a transfer in the adsorbed phase.

Mass balance equations relative to the Model III.

The mass balance equations for this mode are written as follows:

$$-D_{Ads}\,\rho_0\frac{\partial^2 C}{\partial y^2} - D_V\frac{\partial^2 \rho}{\partial y^2} + \rho_0\frac{\partial C}{\partial t} + \varepsilon\frac{\partial \rho}{\partial t} = 0 \qquad (9)$$

where ε represents the global porosity of the solid and:

$$C = f(\rho) \qquad (10)$$

The equation (10) expresses the thermodynamic equilibrium between the gaseous and the adsorbed phases.

The initial conditions are given by:

$$\text{at} \quad t = 0 \quad C = C_1 \quad \text{and} \quad \rho = \rho_1 \qquad (11)$$

The boundary conditions are written:
at

$$y = 0 \qquad \frac{\partial C}{\partial y} = \frac{\partial \rho}{\partial y} = 0 \qquad (12)$$

$$\text{at} \qquad y = e/2 \qquad C = C_2 = f(\rho_2) \qquad \text{and} \qquad \rho = \rho_2 \qquad (13)$$

The sample mass at any instant *t* is evaluated by the relation:

$$m(t) = m_0 + 2\ S \int_0^{e/2} \rho_0\ C(t)\ dy + 2\,S\varepsilon \int_0^{e/2} \rho(t)\ dy \qquad (14)$$

The contribution of the third term of the equation (14) is always very weak comparing to the two other terms.

Mass balance equations relative to the Model IV.
The mass balance equations of the last model leads to the equations:

$$-D_{Ads}\ \rho_0 \frac{\partial^2 C}{\partial y^2} + \rho_0 \frac{\partial C}{\partial t} + \rho_0\ ka\ (C - f(\rho)) = 0 \qquad (15)$$

$$-D_V \frac{\partial^2 \rho}{\partial y^2} + \varepsilon \frac{\partial \rho}{\partial t} - \rho_0\ ka\ (C - f(\rho)) = 0 \qquad (16)$$

The initial and boundary conditions are identical to Model III conditions and are given by the equations (11-13). The sample mass at any instant *t* is evaluated by the la relation (14).

Numerical resolution.
The differential equations presented in the previous section introduce partial derivatives with respect to the space ($\partial(\ )/\partial y$) and with respect to the time ($\partial(\ )/\partial t$). These equations are solved by the finite difference method. The procedure for deriving finite difference equations consists of approximating the derivatives in the differential equations via a truncated Taylor series. The integration domain is recovered by a regular grid of points. The distance between two grid points is defined by:

$$y = \frac{e/2}{M+1} \qquad (17)$$

where *M* is the grid points number.

$$C_n^i = C(y_i, t_n) \quad (18)$$

C_n^i kg A.kg^{-1} porous solid on the grid point *i*, distanced by $y_i = i\,\Delta y$ from the pellet center at the instant tn=ndt; *dt* is the integration time step and *n* is the number of the integration time steps. The partial derivatives with respect to the time and the space take the form (Eq. 19, 20):

$$\frac{\partial C_n^i}{\partial t} = \frac{C_{n+1}^i - C_n^i}{dt} \quad (19)$$

$$\frac{\partial^2 C_n^i}{\partial y^2} = \frac{C_n^{i+1} - 2C_n^i + C_n^{i-1}}{y^2} \quad (20)$$

The four presented models are approximated to a parabolic form equation.

A regular grid with 10^4 grid point has been used for the following simulations. The run time varies according to of the models between few minutes to two hours.

Numerical simulation and results

It is interesting to compare the numerical results obtained with the proposed four models and experimental data in order to investigate if the representation of the real phenomena improves the simulation. Experimental data giving the diffusion coefficients keep rare in the literature. An experimental study of desorption of water from a wood sample (Mouchot and Zoulalian 2005) allowed us to realize the described comparison. The experiments are carried out with beech wood. During the experimental study, tests of humidification and drying were realized. The samples used for these measures have been selected in such manner that diffusion transfer takes place in one only orthotropic direction. The wood is previously placed in a surrounding humid air at a fixed temperature (35°C), characterized with a relative moisture Cg_1 (kg water. kg^{-1} dry air) still the attainment of the thermodynamic equilibrium. The initial wood moisture is then well known. The desorption experience consist on placing the samples in isothermal conditions (35°C) in an enclosure with a constant relative moisture Cg_2 such that $Cg_2 < Cg_1$. A desorption diffusion transfer of water from the wood sample towards the gas phase of the enclosure results. The mass of the sample decreases during the time until a new thermodynamic equilibrium corresponding to moisture Cg_2 is established. During the desorption experiences the mass variations of the wood sample with respect to the time have been registered. The Model III needs $C = f(\mathrm{r})$ an expression giving the wood moisture *C* in equilibrium with the surrounding air moisture *Cg* for a given temperature, keeping in mind also that ρ = *f(Cg)*. Several correlations are available in the literature (Lartigue and Puiggali 1987, Bastias and Cloutier 2005), but all these correlation do not give a good prediction of the wood moisture for the experimental temperature 35°C. In order to resolve this problem we have used an experimental abacus (Siau 1995) giving the values of C as a function of the surrounding air moisture at 35°C. The equilibrium relation $C = f(\mathrm{r})$ was plotted and gifts the following polynomial form:

$$C = 3\,10^6\ \rho^4 - 286811\ \rho^3 + 9326.2\ \rho^2 - 129.74\ \rho + 0.721 \quad (21)$$

The evolution of the sample weight obtained experimentally and numerically is shown on Figs. 2-10. A non-dimension variable E was used:

$$E = \frac{m - m_{final}}{m_{initial} - m_{final}} \qquad (22)$$

were :

-m_{final} is the sample weight in equilibrium with the humidity C_2;
-$m_{initial}$ is the sample weight in equilibrium with the humidity C_1;
-m is the current sample weight at the instant t.

The geometric characteristics of the wood samples and the measured diffusion coefficients for the adsorbed water and the vapor water are given in Table 1. The choice of the samples is done according to the following criteria: in the first experience HL11, the water transport is done in the axial direction, in the second one H7T, the water transfer occurs in the tangential orthotropic direction of the wood.

Table 1: Geometric characteristics and diffusion coefficients for samples HL11 and H7T.

Sample name	e (mm)	r_B (kg m^{-3})	S (mm^2)	D_V (m^2 s^{-1})	D_A (m^2 s^{-1})	D^* (m^2 s^{-1})
HL11	19,0	786,1	4043,2	3,3 10^{-6}	3,38 10^{-10}	1,05 10^{-9}
H7T	12,6	736,0	4128,1	3,7 10^{-8}	1,64 10^{-11}	8,13 10^{-11}

Numerical results obtained using the Model I, Model Ia.

The comparison between the experimental data and the numerical results obtained by the Model I are shown on the Fig. 2 (sample HL11) and Fig. 3 (sample H7T). It can be seen that with the optimized value of D^* the model represents correctly the experimental curves. In order to investigate the efficiency of the Model Ia, we have realized several simulations using different values of h_m, hoping to obtain some differences with the results obtained by the Model I. In real conditions, the motion of the gaseous phase is characterized with values of h_m close to 10^{-3} m s^{-1}. The results obtained with the Model I, the Model Ia (for $h_m = 10^{-3}$ m s^{-1}, and $h_m = 5.10^{-7}$ m s^{-1}) and the experimental data are presented on the Fig. 4. The analysis of this comparison allows us to conclude that external mass transfer resistance can be neglected for this experience.

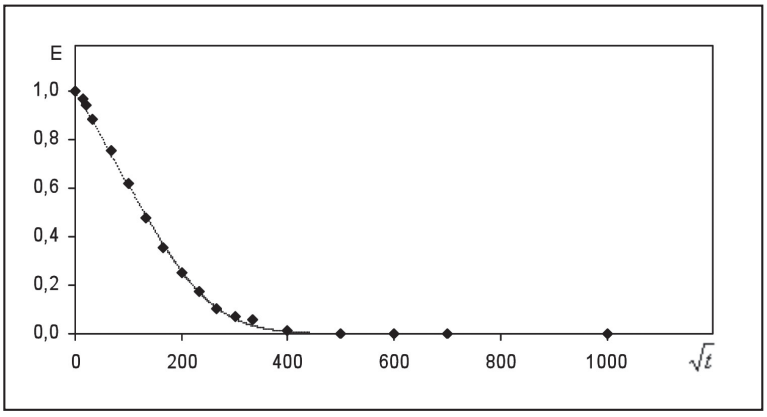

Fig. 2. Comparison between the experimental data and the simulation results obtained using Model I for the sample HL11 (♦ : experimental data, - - - - - : numerical results).

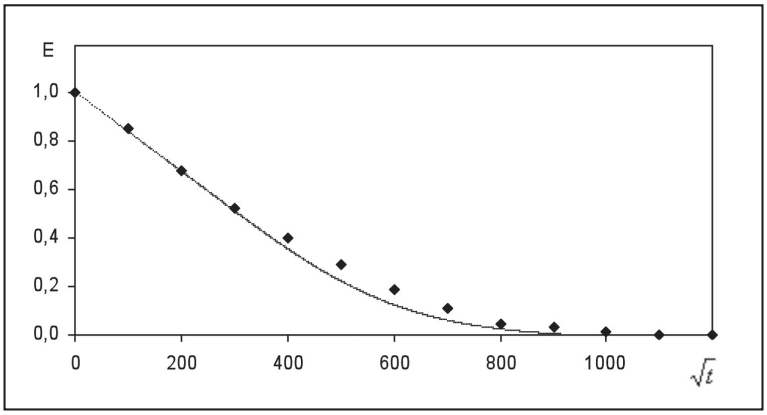

Fig. 3. Comparison between the experimental data and the simulation results obtained using Model I for the sample H7T (♦ : experimental data, - - - - - : numerical results).

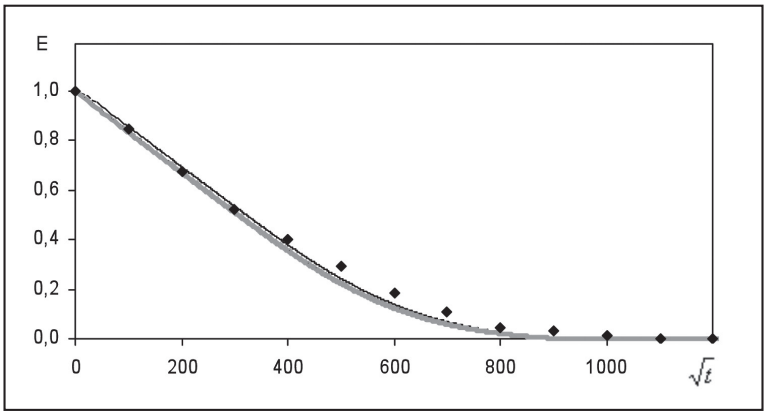

Fig. 4. Comparison between the experimental data and the simulation results obtained using Model I and Model Ia for the sample H7T (♦ : experimental data, - - - - : numerical results using Model I, —— numerical results using Model Ia with $k_C = 10^{-3}\ m\ s^{-1}$, --- numerical results using Model Ia $k_C = 5.10^{-7}\ m\ s^{-1}$).

Numerical results obtained using the Model II.

The numerical simulation realized using the Model II and the experimental value of the diffusion coefficient in adsorbed phase D_{Ads} does not give a good representation of the experimental data (see Figs. 5, 6). This simulation confirms that the adsorption process could not be reduced to the mass transfer in the adsorbed phase.

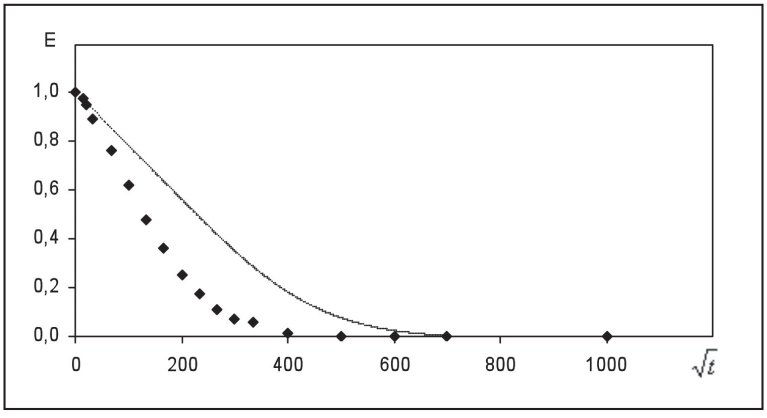

Fig. 5. Comparison between the experimental data and the simulation results obtained using Model II for the sample HL11 (♦ : experimental data, - - - - - : numerical results).

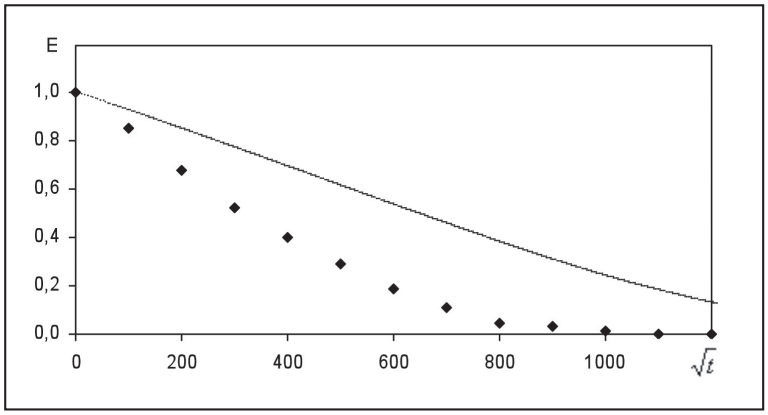

Fig. 6. Comparison between the experimental data and the simulation results obtained using Model II for the sample H7T (♦ : experimental data, - - - - - : numerical results).

Numerical results obtained using the Model III.

This model takes into account the simultaneous diffusion mass transfer in the adsorbed phase and the gaseous phase, assuming the existence of thermodynamic equilibrium between the two phases. The fluxes are characterized respectively with the diffusion coefficients D_{Ads} and D_V and the thermodynamic equilibrium at 35°C is introduced using Eq. 21. The numerical results obtained with the Model III (Figs. 7, 8) are not satisfying. That means that the hypothesis of a thermodynamic equilibrium is not always justified.

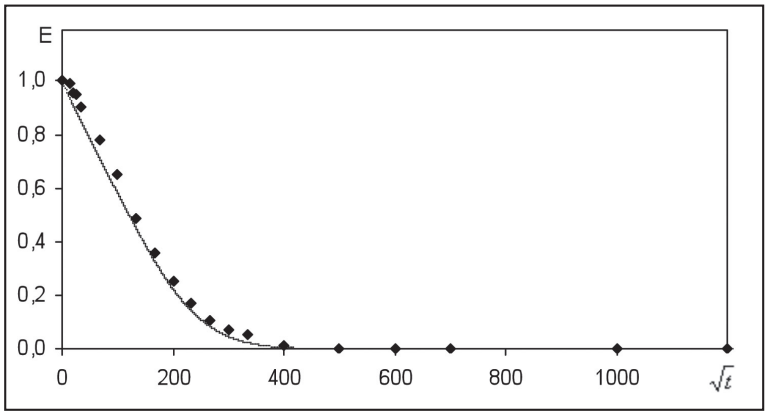

Fig. 7. Comparison between the experimental data and the simulation results obtained using Model III for the sample HL11 (♦ : experimental data, - - - - - : numerical results).

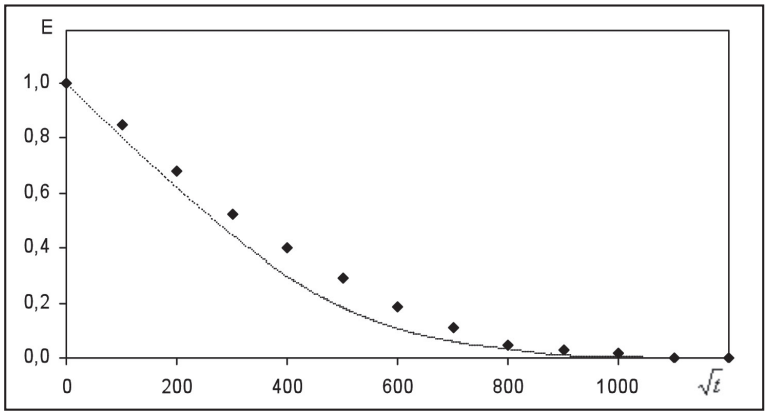

Fig. 8. Comparison between the experimental data and the simulation results obtained using Model III for the sample H7T (♦ : experimental data, - - - - - : numerical results).

Numerical results obtained using the Model IV.

The Model IV uses the experimental values of the diffusion coefficients in adsorbed gaseous D_V and in the adsorbed phase D_{Ads} and needs also the knowledge of the global volume transfer coefficient *ka*. In this study *ka* is determined by optimization, searching for minimize the error function (Eq. 23).

$$error = \frac{1}{N}\sum_{N} 2\left|\frac{m_{\exp} - m_{cal}}{m_{\exp} + m_{cal}}\right| \qquad (23)$$

where m_{exp} is the sample weight obtained experimentally and m_{cal} is the calculated value of the sample weight. The values found for the global volume transfer coefficient *ka* are as respectively 2.7 10^{-2} s^{-1} for the sample HL11 and 2.3 10^{-2} s^{-1} for the sample H7T. So, if the properties of the diffusionnel transfer in the two samples are different the values found for *ka* are very close. That confirms that transfer resistance at the wood fiber between the gaseous and the adsorbed phase does not depend on the transfer direction, and confirms the assumption that the fiber composition is isotropic. The comparison between the experimental and the numerical results are given of the Figs. 9, 10. It can be seen that the numerical simulation is very satisfying. Same if the simulation results obtained using the Model I are also very good, it does not allow to represent the real mass transfer phenomena which include the simultaneous diffusion fluxes in gaseous and adsorbed phases and a resistance transfer between gaseous and adsorbed phases.

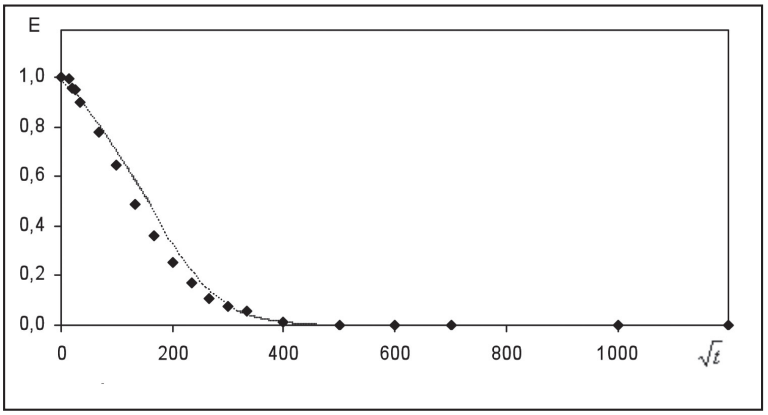

Fig. 9. Comparison between the experimental data and the simulation results obtained using Model IV for the sample HL11 (♦ : experimental data, - - - - - : numerical results).

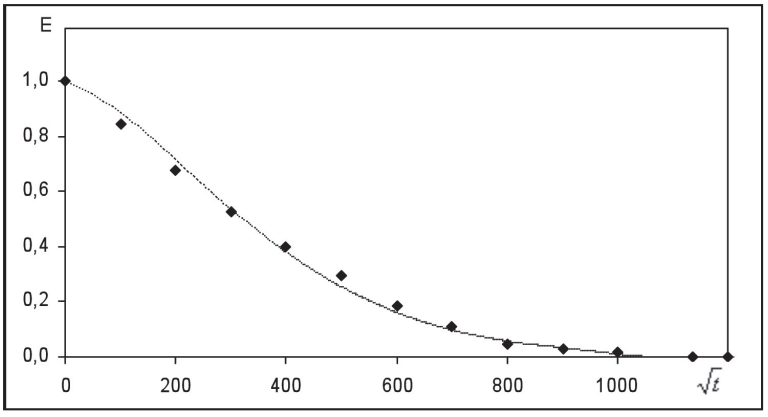

Fig. 10. Comparison between the experimental data and the simulation results obtained using Model IV for the sample H7T (♦ : experimental data, - - - - - : numerical results).

CONCLUDING REMARKS

The comparison between the numerical results obtained using the model which takes into account the simultaneous diffusion of water in the gaseous and adsorbed phase shows a good agreement with the experimental data. The Model I permits to represent also the experimental curves but the diffusion coefficient obtained by optimisation remains different from the values deduced of appropriate experiments for their evaluation. The study of two wood samples proves that the thermodynamic equilibrium between the gaseous and the adsorbed phase is not necessarily established. It has to be reminded that the equilibrium condition is generally admitted when the usual industrial absorbent are studied (active carbon, zeolites…).

REFERENCES

Bastias, M. V.; Cloutier, A. 2005. Evaluation of wood sorption models for high temperatures. *Maderas Ciencia y tecnología* 7(3):145-158.

Do, D. D. 1998. Adsorption analysis: Equilibria and kinetics. London: Imperial College Press.

Do, H. D.; Do, D. D. 1998. Maxwell-Stefan analysis of multicomponent transient diffusion in the capillary and adsorption of hydrocarbons in activated carbon particle. *Chemical Engineering Science* 53 (6): 1239-1252.

Glueckauf, E.; Coates, J. E. 1947. Theory of chromatography IV. *Journal Chemical Society* 1315-1321.

Lartigue, C.; Puiggali, J. R. 1987. Caractéristiques des pins des Landes à la compréhension des phénomènes de séchage. 2ème colloque Sciences et Industries du Bois. ARBOLOR, Nancy, France. 57-64.

Mouchot, N.; Zoulalian, A. 2005. Détermination des caractéristiques diffusionnelles de transfert d'un soluté gazeux adsorbable au sein d'un milieu poreux. Application au cas de la vapeur d'eau au sein du bois de hêtre. *The Canadian Journal of Chemical Eng* 83: 328-335.

Mugge, J.; Bosch, H.; Teith, T. 2001. Measuring and modeling gas adsorption kinetics in single porous particles. *Chemical Engineering Science* 56 (18): 5351-5360.

Ruthven, D.M. 1984. Principles of adsorption and adsorption processes. New York: Wiley.

Siau, J. F. 1995. Wood: influence of moisture on physical properties. Department of Wood Science and Forest Products, Virginia Polytechnic Institute and State University.

Yang, R. 1987. *Gas separation by adsorption processes*. Boston: Butterworths Series in Chemical Engineering.

Nomenclature

A	transferred constituent
C	solid phase concentration kg A.kg^{-1} porous solid, [-]
Cg	gas phase concentration kg A.kg^{-1} vector gas), [-]
D_{Ads}	apparent diffusivity in the adsorbed phase, m^2 s^{-1}
D_V	apparent diffusivity in the gaseous phase, m^2 s^{-1}
D^*	apparent diffusivity obtained by optimization of the Model I, m^2 s^{-1}
e	sample thickness, m
ka	global volume transfer coefficient, s^{-1}
h_m,	external mass transfer coefficient, m s^{-1}
m	porous solid weight, kg
m_0	porous solid weight before adsorption, kg
t	time, [s]
symbols	
ε	global porosity of the solid, [-]
ρ	density of A in the gaseous phase, kg.m^{-3}
ρ_0	density of solid before adsorption, kg.m^{-3}
φ	mass flux of transferred A, kg s^{-1}